Advanced Materials Technologies

Flexible and Stretchable Electronics for Harsh Environmental Applications

--Manuscript Draft--

Manuscript Number:	admt.201900145R2
Full Title:	Flexible and Stretchable Electronics for Harsh Environmental Applications
Article Type:	Invited Review
Section/Category:	
Keywords:	marine ecology; flexible electronic; stretchable electronic; harsh environment.
Corresponding Author:	Muhammad Mustafa Hussain, Ph.D. King Abdullah University of Science and Technology KAUST Thuwal, SAUDI ARABIA
Additional Information:	
Question	**Response**
Please submit a plain text version of your cover letter here.	Dear Dr. Jiang, Thank you for the kind opportunity to revise our manuscript. We have carefully addressed the concerns raised by Reviewer 1. However, we would like to point out that we have intentionally skipped implantable electronics as that itself represents and deserves an independent focused review on that. Hope you will find the current version readily acceptable to ADMT. Thank you in advance. Muhammad
Do you or any of your co-authors have a conflict of interest to declare?	No. The authors declare no conflict of interest.
Corresponding Author Secondary Information:	
Corresponding Author's Institution:	King Abdullah University of Science and Technology KAUST
Corresponding Author's Secondary Institution:	
First Author:	Amani Almuslem, MSc
First Author Secondary Information:	
Order of Authors:	Amani Almuslem, MSc
	Sohail Faizan Shaikh, MSc
	Muhammad Mustafa Hussain, Ph.D.
Order of Authors Secondary Information:	
Abstract:	Monitoring, measuring and controlling electronic systems in space exploration, automotive industries, downhole oil and gas industries, oceanic environment, geothermal power plants, etc. require materials and processes that can withstand harsh environments. Such harshness can come from the surrounding temperature, varying pressure, intense radiation, reactive chemicals, humidity, salinity, or a combination of any of these conditions. Here, we review recent progress in the development of flexible and stretchable electronic devices for harsh environment applications. We consider studies on how the selection of a specific material is important for a specific application and how the selection of the material plays critical role in sustained performance. We present specific examples for selected applications. We also look at works on methods and designs for achieving flexibility and stretchability in devices designed for harsh environments. Finally, we look at studies on

	packaging techniques that enable deployment of conventional electronic devices in harsh environment applications and offer a few examples.

Powered by Editorial Manager® and ProduXion Manager® from Aries Systems Corporation

Revised Manuscript

DOI:
Article type: Review paper

Title: Flexible and Stretchable Electronics for Harsh Environmental Applications

Amani S. Almuslem[1], Sohail F. Shaikh[1], Muhammad M. Hussain[1]*

[1]mmh Labs, Electrical Engineering, Computer Electrical Mathematical Science and Engineering Division, King Abdullah University of Science and Technology (KAUST), Thuwal 23955-6900, Saudi Arabia

[*]EECS, University of California, Berkeley, CA 94720, USA

*Corresponding author's e-mail: muhammadmustafa.hussain@kaust.edu.sa

Keywords: marine ecology; flexible electronic; stretchable electronic; harsh environment.

Abstract

Monitoring, measuring and controlling electronic systems in space exploration, automotive industries, downhole oil and gas industries, marine environment, geothermal power plants, etc. require materials and processes that can withstand harsh environments. Such harshness can come from the surrounding temperature, varying pressure, intense radiation, reactive chemicals, humidity, salinity, or a combination of any of these conditions. Here, we review recent progress in the development of flexible and stretchable electronic devices for harsh environment applications. We consider studies on how the selection of a specific material is critical for a particular application and how the selection of the material plays a critical role in sustained performance. We present certain examples for selected applications. We also look at works on methods and designs for achieving flexibility and stretchability in devices designed for harsh environments. Finally, we look at studies on packaging techniques that enable deployment of conventional electronic devices in harsh environment applications and offer a few examples.

1. INTRODUCTION

Electronic devices used in harsh environments must be designed to withstand extremely low or high temperatures, high radiation, high salinity, high humidity, or any combination of these conditions. Although the temperature is only one of the possible determinants of a harsh environment, it serves as a good example of the types of harsh environments that electronics can encounter. Commercially available complementary metal oxide semiconductor (CMOS) integrated circuits (IC) are designed for temperatures ranging from 0 °C to 85 °C, whereas military-grade ICs are expected to withstand temperatures from -55 °C to 150 °C. Temperatures beyond these ranges can be considered as harsh environments for standard CMOS devices. Temperature as low as -246 °C is encountered in deep space exploration. Electronic devices used on manned or unmanned spacecraft must be designed to withstand deep cryogenic conditions. On the other hand, high temperatures are commonly encountered by electronics systems in automotive engines used on earth and in aerospace electronics systems where operating temperatures could reach up to 500 °C. Other high-temperature environments where electronics are often used include oil and gas wells and geothermal wells in which the electronics must operate reliably at temperatures between 250 °C and 300 °C.

Although silicon is fundamental to 90% of the electronics devices currently produced, its unstable material properties under harsh conditions restrict its use in harsh environments. The change in the electrical properties of silicon is more pronounced when compared with other properties (magnetic/optical/mechanical/thermal) under increased temperature. Elevated temperatures generate increased intrinsic carriers and the temperature at which these intrinsic carriers start to increase depends on the band gap of the material as shown in the following equation:

$$n_i = \sqrt{N_c N_v} e^{\frac{-E_g}{2KT}} \quad , \qquad (1)$$

where $\boldsymbol{n_i}$ is the intrinsic carrier concentration, $\boldsymbol{N_c}$ and $\boldsymbol{N_v}$ are the effective density of states in the conduction band and valence band, respectively, $\boldsymbol{E_g}$ is the energy gap of the material, $\boldsymbol{K}$ is Boltzmann's constant, and $\boldsymbol{T}$ is the absolute temperature. When the intrinsic carrier becomes dependent on temperature, the performance of the material is unreliable at elevated temperatures. When the intrinsic carriers exceed the extrinsic carriers, the p-n junctions fail. In this case, the band gap of the material can indicate the tolerable operating temperature and the thermal tolerance of the system.[1] This means that other wide band gap and robust materials should replace Si in electronics when they are designed for high temperatures. Table 1 summarizes the maximum recommended operating temperatures of electronic devices fabricated using different semiconducting materials and the maturity level of the respective technologies made from these materials.[2]

The development of flexible and stretchable electronic devices has advanced quickly. Flexible and stretchable electronics are designed to withstand repeated 2D/3D mechanical deformation while maintaining their performance(s). As such, they lend themselves well to applications in harsh environments. Here, we review recent progress in the development of flexible and stretchable electronics for harsh environments by highlighting the selection of the best materials for the conditions (section 2), design and fabrication processes (section 3), suitable packing techniques (section 4), and future challenges and insights (section 5).

2. OPTIMAL MATERIALS FOR HARSH ENVIRONMENTS

Long-term device performance is correlated with the material and the surrounding environment. Finding the optimal material for a particular application requires consideration of

the surrounding environmental conditions. Table 2 summarizes the environmental variables that are experienced in these fields. [3–11] Every material has a feature that defines its limitation in a harsh environment (band gap energy, inter-atomic bonding, breakdown field, carrier mobility, crystal structures, and existing defects). [12–14]

A material can be inherently resistant to an aggressive environment or it can be tailored to overcome the hostility in the environment by means increases more elevated in non-inert chemical environments, like saline, acidic, or alkaline media, and in presence of reactive gases, such as chlorine, fluorine, hydrogen sulfide, and carbon monoxide. Conductive metallic materials form the core of any electronic device, whether it is in a rigid, flexible, or stretchable form. Instability of the metallic interconnects not only deteriorates the device's performance but also leads to system failure over time. Hence, it is critical to choose the most suitable metal for a specific harsh environment. Metals and their alloys, such as Nickel (Ni), Aluminum (Al), Copper (Cu), Zirconium (Zr), Tantalum (Ta), alloyed steels, and Titanium (Ti) alloys, demonstrate excellent stability and their surfaces remain corrosion-free in the presence of acids. The superiority of Al, Ti, and Cr and their alloys is due to surface oxidative stability, which resists the corrosion caused by strongly oxidizing acidic environments. [14,15] In addition to these conductive materials, graphene has been known to exhibit remarkable properties like high thermal stability, high mechanical strength, and distinctive electrical conductivity, in addition to its attractive features of inherent flexibility and transparency. [16–19]

The following points should be considered in selecting a material for an application in a specific harsh environment: i) the abundance of the material and cost, ii) compatibility with well-established CMOS technologies and ease of integration, and iii) required (optical, thermal, mechanical, electrical, or magnetic) properties. The functionality of the device at elevated

temperature deteriorates faster if an inappropriate material is chosen, which can be observed in high substrate leakage current, low carrier mobility, minimal dielectric breakdown strength, and generated electro-migration of metal atoms causing the alteration in the device's key parameters as reported by Watson *et al*. [20]

Materials for fabricating flexible electronics for harsh environment applications can be either inherently flexible due to the specific material structure, as in zero-dimensional (0D) materials, one-dimensional (1D) materials (such as nanowires and nanotubes), or two-dimensional (2D) materials like graphene sheets. Or the conventional materials like Si or metals can be processed/engineered to imbibe flexibility in the electronic devices. Polymers and elastomers that are naturally flexible have also been used as substrates and active materials in flexible electronics. However, the electronics with polymeric active materials are inferior in performance to be considered for any real life applications. On the other hand, polymers as sensing and substrate materials are widely used. Conventional materials that are rigid are processed to obtain flexible counterparts mainly by using a volumetric thickness reduction technique. Various such techniques include transfer printing, the trench-protect-release (TPER) based process, double transfer printing, soft-etch-back (SEB), corrugation architecture, silicon-on-insulator (SOI), and laser lift-off process. [21–35] The practical advantages of making materials flexible include ability to deploy on a complex and asymmetrical surfaces, enhancing device performance due to excellent and proven conventional superior properties matching with the current state-of-the-art rigid device technologies, in addition to reducing the form factor which implies low weight and low cost due to new and easy fabrication processes.[36,37]

Any free-standing material that is less than 100 nm in one of its three spatial dimensions can be inherently flexible and is often termed a nanomaterial. The most prominent examples of

nanomaterials include lower dimension zero-dimension (0D), 1D, and 2D materials. 1D material includes nanotubes and nanowires, whereas 2D materials include atomic crystal structure material such as graphene and dichalcogenide materials. Although the flexibility in nanomaterials is inherently present due to their ultra-thinness, their resistance to environmental stress depends on the material's chemical composition. For example, nanoceramic material, such as silicon carbide (SiC)-based nanofibers and gallium nitride GaN-based nanowires, exhibit inherent flexibility and required stability under extreme conditions.

2.1. Silicon Carbide (SiC)

Silicon, silicon on insulator (SOI), or silicon germanium are suitable choices for moderate environments; the advanced semiconductor material silicon carbide works well under harsher conditions. The very low intrinsic carrier concentration, wide bandgap, and high breakdown electric field make SiC an excellent choice for high-temperature environments. The maximum operating temperature for SiC devices is 800 °C that covers a vast majority of harsh environments. Wang *et al.* demonstrated that inherently flexible SiC ceramic nanofibers can be used as an electromagnetic wave absorber under extreme condition involving high temperatures up to 500 °C in an aggressive alkaline environment. [38] The extreme flexibility of the fabricated device was reported in terms of bending angles up to 142.6° as can be seen in Figure 1a. SiC ceramic nanofibers are synthesized using electrospinning followed by high-temperature heat treatment. This technique allows better diameter control compared with other methods and results in a flexible material. The SiC nanofibers exhibit a high contact angle up to 140.05, indicating an excellent hydrophobic surface due to the surface topology of SiC and the presence of C−C and C═C functional groups. Wang *et al*. also explored the imperative dielectric and magnetic parameters in determining the utility and applicability of the material to absorb

electromagnetic waves. Based on the dielectric value, SiC nanofibers demonstrated high absorption at low frequencies Figure 1(b, c). [38]

2.2. SiC Nanowires

Nanowires are another example of inherent flexible materials used in applications for harsh environments because it is capable of tolerating cyclic mechanical deformation with extraordinary characteristics in terms of flexibility and stretchability. Among current nanostructure materials, SiC nanowires are widely used due to their desired physical properties, such as excellent thermal conductivity, high thermal stability, high stiffness and strength, and chemical resistance. [39–41] Sun *et al*. successfully synthesized a flexible, transparent, and freestanding 2H-SiC nanowires fabric (FTS-NWF) for photo-absorbers and photo-detectors under harsh conditions. Chemical vapor deposition exploiting airflow-oriented growth few planar stacking faults. This material demonstrated photo-switching characteristics, as it was transparent to the visible spectral range (380–780 nm) and opaque to the UV spectral range (200–380 nm). The electrical characteristics of an FTS-NWF-based two-terminal device were shown by negligible changes in output under repetitive mechanical cyclic deformation. [42]

2.3. Gallium Nitride

To overcome several limitations in low bandgap energy semiconducting materials, scientists have explored a new generation of materials by combining column-III elements with nitrogen, providing III-nitride materials, including aluminum nitride (AlN), indium nitride, and gallium nitride (GaN). GaN has been extensively studied due to its high-voltage operation capabilities, low resistive loss and wide range of operating temperatures. GaN nanowires grown directly on the flexible metal foil can serve as an inherent flexible material platform. [43–45] May *et al.* recently presented a flexible LED fabricated from GaN nanowires grown directly on metal foil

using molecular beam epitaxy (MBE) for use in hostile environments. [46] The nanowire structure not only exhibited flexibility but also successfully tackled the large strain originating from the lattice mismatch in conventional thin film material platforms due to the large surface-to-volume ratio of the nanowire. This hallmark enabled materials with different lattice constants to be tailored without high dislocation densities and resulting in excellent device performance. The optical properties of nanowires grown on flexible metal foil and rigid Si are similar to those obtained from GaN nanowires in foil grains despite the variation in growth angle and density. Additionally, an LED with tunnel junction architecture was fabricated by May *et al.* using AlGaN grown on Ta foil as an active material. It demonstrated a turn-on voltage similar to that obtained from the same device built on a Si substrate. [46]

Calabrese *et al*. also grew GaN nanowires on flexible Ti foil. Their single crystalline GaN nanowire, vertically stacked, N-terminated, and uncoalesced wurtzite GaN structure was grown on flexible Ti foil using plasma-assisted molecular beam epitaxy. [47] The crystallinity degrees of nanowires grown on Ti foil and Si were identical. The absence of coalescence in the nanowire grown on Ti foil is advantageous over that grown-on Si. The mechanical deformations of the substrate have no effect on the room-temperature photoluminescence spectrum of the nanowire under a small radius of curvature up to 4 mm. Furthermore, no separation was reported between the nanowire and Ti foil during bending, indicating excellent mechanical stability. [47]

Boosting Inherent Properties

To boost the properties of interest, some inherent flexible materials can be subjected to certain processes. For example, flexible nanocarbon-paper-based lighting developed by Bao *et al.* was subjected to a two-step reduction process to enhance its conductivity by converting the nanocarbon paper to a highly graphitic form. [48] The process resulted in fairly reduced-graphene-

oxide (RGO) paper, which is mixed with carbon nanotubes (CNTs) to eliminate defects to achieve the desired crystallinity of graphene. These modifications in nanocarbon paper (RGO-CNT) allowed the material to withstand high temperatures up to 3000 K and to fulfill the requirements of lighting according to the Stefan–Boltzmann law. The thermal stability test at 2000 K in a vacuum demonstrated the superiority of RGO-CNT over other nanocarbon-based papers over a period beyond 50 hours. The RGO-CNT paper exhibited extraordinary flexibility characteristics by deforming into different shapes and configurations using diverse and affordable fabrication methods as depicted in Figure (2a-c). [48]

Similarly, incorporating SiC nanowires (SiC NW) in reduced graphene oxides (rGO) has been reported to maintain the favorable characteristic of electromagnetic wave absorbers, such as lightweight, reduced thickness, and increased strength without compromise the flexibility Figure 2-d. [49] The practical electromagnetic wave absorber has a trade-off between high absorption properties and impedance matching with free space, whereas the absorption capability is correlated with the dissipation of the electromagnetic wave power inside the absorbent material (a function of the permittivity, ε, and permeability, μ, of the absorbent material). A study on the dielectric loss of rGO foam and S-60, S-120, and S-180 (where 60, 120, 180 refer to the reacted time in min of silicon/silica powder and rGO to prepare rGO/SiC NW foams) demonstrated frequency-dependent behavior. Additionally, the maximum effective permittivity was measured for S-180 (which had high SiC nanowire content), suggesting the major role played by SiC nanowires in boosting the dielectric loss of absorbent material and leading to better absorption capabilities Figure 2e. Similarly, comparing the reflection loss of rGO foam and S-60, S-120, and S-180 revealed the superiority of S-120 as an electromagnetic wave absorbent material with minimal reflection loss and more importantly retention of the balance between dielectric loss and

impedance matching with the free space. [49] Hence, introducing process or composite materials can boost and tune the properties of a material to a good extent.

Furthermore, the development of a hybrid material structure for enhancing mechanical and electrical properties simultaneously boosting the stability of material under the working environment presents a pragmatic approach. Recently, Li *et al*. demonstrated a hybrid structure of graphene and aligned silver nanowires as the functional material for a transparent deformable heater for wearable electronics applications. Such hybrid structure and composition of graphene and aligned nanowires resulted in drastic performance improvements like low power consumption, higher saturation temperature, efficient heat distribution, high thermal resistance, less heat dissipation, having relatively high transmittance. The stability of the hybrid structure was demonstrated by sustained electrical property changing insignificantly over 1000 bending cycles. [50]

Similarly, in variety of applications, resistance to oxidation of the functional material is of great importance as it deteriorates the performance to a great extent and in many cases, degrades the performance in an irreversible manner to be non-functional anymore. [51] For instance, copper nanowires have several mechanical advantages over other conventional metals used in wearable electronic due to its endurance, however, its weak oxidation resistance hinders the ubiquitous usage of copper and copper nanowires in a majority of flexible electronics applications.[52] Kim *et al*. have recently illustrated a new way to synthesize copper nanowire leading to better control of nanowire morphology along with high yield production to tackle the issues related to the usage of copper nanowire described above. In this study, the most important property of oxidation resistance was enhanced by the application of 15 μm thick polyurethane acrylate (PUA) resin coating on nanowires. This technique helped in getting highly transparent,

mechanically flexible, chemically stable (against oxidation), and electrically conductive superior copper nanowires. Although the exposure to the surrounding environment of these coated nanowires showed a 15% increase in resistance within a day, it saturated after that until the entire period of the experiment. On the contrary, the samples that were not coated with the PUA oxidation resistive coating showed continuous increasing electrical resistance as a result of weak oxidation resistance. Thus, the coated Cu nanowires were successfully used as cheap electrode material for a clear bendable capacitive force detection touch sensor pads.[53]

In the same domain of controlling and enhancing the oxidizing stability of copper nanowires, Shi *et al.* presented another approach of using graphene coating as an oxidation preventive layer. Unlike the PUA resin coating, this method of coating a graphene-layer has shown no deterioration even after extended exposure to the oxidizing environment for up to 6 months.[54] Likewise, most of the metallic thin films get oxidized at a high temperature leading to deviation from the required functions due to cracks and alteration in resistance. [51,55] Hence, a protective layer is essential to sustain the properties even at elevated temperatures. For elevated temperature environment, Seifert *et al*. investigated the stability of 110 nm thin Ru-Al based thin film against the oxidation in air and vacuum as well by introducing a 20 nm thin SiO_2 or Al_2O_3 layer coating. The stability tests were performed by annealing the coated Ru-Al based thin film at 900 °C for 10 hours in the air and high vacuum (less than 10^{-8} bar) and compared with uncoated Ru-Al thin films. The vacuum had no oxidizing effect on the hybrid material stack of Ru-Al for both coated and uncoated samples, however, the oxidation resistance of SiO_2 coated Ru-Al was higher than that of Al_2O_3 coated film which failed to prevent oxidation at a temperature beyond 800 °C.[56]

The material selection for the contacts in any application relies beyond its oxidation resistance specifically to be operational at elevated temperatures in many applications. In such

applications, the intended material must have a high melting point, high electrical conductivity, and adequate corrosion resistance. [57–59] Demonstration of Pt as a material for establishing contacts with the electronic interface using wedge-bonding technique has promised a great deal for the future research activities by Brachmann *et al*. The study has successfully demonstrated usage of wedge bonding using Pt on a 1 μm thick Pt-based-antenna and the pads of a surface acoustic sensor for wireless temperature sensing (>600ºC). The gap between metal bond and the pad in wire bonding and wedge-bonding are generally caused by poor bonding strength beside low melting temperature, which was overcome by using Pt as material for bonding.[60]

The recent development of atomic layer deposition (ALD) technique and variety of tools to obtain extremely dense, high quality and conformal thin films with excellent control over the thickness, has attracted amazing applications in barrier coatings and passivation materials for electronics devices stability. Many of the films deposited using ALD are highly dense and the uniform which prevents gas permeability and becomes a barrier for moisture against the thin layer. Utilizing such techniques with considerable care is necessary for an aggressive medium to retain chemical stability.[61,62] Singh *et al*. studied the chemical stability of a variety of thin films deposited by low-temperature plasma-enhanced atomic layer deposition technique on a glass substrate coated with 2 nm TiO_2/ 50 nm Au /10 nm Cr. The chemical stability has been examined in this study using electrochemical impedance spectroscopy (EIS) and photoluminescence (PL) methods to investigate different thin films. Among the investigated ALD thin films (Aluminum oxide (Al_2O_3), Hafnium dioxide (HfO_2), Titanium Dioxide (TiO_2), and Zirconium dioxide (ZrO_2)), ALD TiO_2 and ZrO_2 exhibit most stable chemical characteristic in all aggressive ionic chemical mediums including 3.5% NaCl solution, highly saline sea water, hydrochloric acid HCl (pH = 4), and sulfuric acid H_2SO_4 (pH = 4).[60]

In recent years, hydrogels have been very extensively used in point-of-care diagnostics as well as wearable electronics applications. The hydrogel can be used as functional or passive material which is generally thicker due to their conventional synthesis and spreading techniques. Hydrogel refers to a class of polymer material which capable of absorbing water in its mesh and as a result thickness increasing occurs. Optimizing and developing initiated chemical vapor deposition (iCVD) technique enables scaling down the thickness of hydrogel films which result in boosting the sensitivity of the hydrogel film to the moisture and accelerating response time demonstrated recently by Buchberger. [63] The suggestion of optical measurement of the hydrogel expansion as a function of ambient humidity in this work enables the use of hydrogel-based humidity sensor in a harsh application such as a corrosive or explosive environment where no electrical components can be located.

Some materials can self-recover upon exposure to detrimental external factors. [64] Self-recovery enables the effects of hostile factors encountered in the ambient atmosphere to be tackled. A material's self-recovery characteristics upon exposure to humidity are elaborate. Moisture is considered a hostile condition in wearable electronics as it can cause performance degradation. To overcome the effect of humidity, the proper selection of material, packaging, and design is essential. A novel laminated electret cellular film with a unique property of charge self-recovery even upon working in high humidity conditions at an elevated temperature up to 70ºC is an excellent choice for a flexible electrostatic generator that it is intended to work in humid environments. The electrostatic generator's working principle relies on the surplus charges of electret materials generated in electrostatic induction. Neutralizing the surplus charges by the ions in the water in a humid environment cause deterioration of the generator's output. The proposed laminated electret cellular film is capable of recovering the surplus charges upon

exposure to a moist atmosphere. Ethylene vinyl acetate copolymer (EVA) and biaxially oriented polypropylene (BOPP) raw films are used to construct the self-recovery laminated electret cellular film following hot-pressing processes. The laminated electret cellular film is capable of restoring the surface potential on the EVA and BOPP sides of the film to 1.8 kV and 1.1 kV, respectively, under the extreme condition of water submersion, and naturally drying up to 100 times. The laminated electret cellular film tolerates up to 0.65 MPa pressure before breaking, indicating acceptable robustness.[64]

To summarize, selection of functional or passive material for any application including harsh environment depend on several factors such as stability, reliability, mechanical and electrical properties, chemical resistance and resistance to several environmental factors that can change the material composition, phase, structure, shape, or basic/derived properties. Similarly, the next paragraphs give some perspective on the selection of substrate material for such applications.

Harsh Environment Compatible Flexible Substrate Selection

Selecting the optimal material for harsh environments is not limited to the active material the choice of material for the flexible substrate is also important. Selecting the proper flexible substrate can improve device performance by providing excellent thermal dissipation of generated heat from the device. Flexible ceramic yttria-stabilized zirconia (YSZ) is often chosen to serve as a substrate for light emitting diodes (LED). A comparison between flexible (LED) performance on flexible ceramic (YSZ) and polymeric substrate demonstrates the vital role of the substrate in heat management, which in turn boosts LED performance. The appropriate thermal management enables high power operation of flexible LEDs. The flexible ceramic (YSZ) substrate is advantageous over other flexible polymeric substrates due to inherent properties effectively matching the requirements of operating flexible LEDs. These advantages

are not limited to high thermal conductivity only; they extend to mechanical deformation tolerance, chemical, and high-temperature stability up to 1000 °C, and near visible light transparency. Kim *et al.* demonstrated the fabrication of flip-chip light emitting diodes (FC-LEDs) on a sapphire substrate. The structure consisted of a GaN p-n junction including InGaN/GaN multiple quantum wells (MQWs). Polishing the sapphire substrate reduced its thickness to the flexible regime. Then a transferring process was achieved via patterning Au/Sn on both the 40 µm YSZ substrate and on top of the ohmic contacts for p-GaN and n-GaN followed by bonding the YSZ to FC-LED using thermo-compression at 300 °C. The optical characteristic of FC-LED on YSZ and polyimide substrate are almost similar when the injected current is below 10 mA. Increasing the injected current (I > 10 mA) causes intensity degradation of the emitted wavelength corresponding to LED on polyimide in comparison with that on YSZ (Figure 3a-b). Moreover, the emission is shifted towards a longer wavelength. Increasing the temperature of the p-n junction contributes to enhancing non-radiative recombination of the charge carrier and narrowing the bandgap energy, which is observed as a lower peak intensity and a longer emission wavelength, respectively. The shifting in the emitted wavelength of the LED on polyamide is six times greater than that of LED on YSZ substrate when the p-n junction temperature reaches 80 °C due to high current injection, which proves the important function of the YSZ substrate in sinking the self-generated heat of the LED. Both LEDs on polyamide and YSZ show excellent durability characteristics under continuous operation for 50 min at high injected current (I > 100mA) Figure (3-c). [36]

3. DESIGN AND ARCHITECTURES FOR FLEXIBLE ELECTRONICS IN HARSH ENVIRONMENTS

The recent advances in thin film technologies have propelled the usage of thin grown films on rigid substrates. Different techniques are employed to transform this rigid structure into a

flexible one by volumetric thickness reduction of the substrate or releasing the structure and then transferring it onto another flexible carrier. [26,27,29,34,36,65,66] Although there are established processes and techniques applied for obtaining flexible organic and inorganic devices for trivial sensing and other known applications, flexible devices and processes for harsh environmental applications are still in their infancy.

In the following section, we focus on different flexing processes and design architectural for introducing stretchability in the electronics for harsh environment materials for specific applications.

3.1. Flexing Approaches and Design of Stretchable Devices

3.1.1. Transfer Process for flexible GaN

GaN-based high electron mobility transistors (HEMT) are one of the basic blocks of harsh-environment electronics. It is well established that GaN-based HEMT fulfills the requirement of high power and high frequency operating conditions due to its wide bandgap and high carrier mobility. [1] The efficient performance can be extended to the flexible configuration of GaN-based HEMT. Mhedhbi *et al.* demonstrated that flexible GaN-based HEMT can be used as a microwave power transferring device. [67] GaN-based HEMT is fabricated on (111) Si substrate and then transferred to adhesive flexible tape. The transferring method starts with protecting the device with a thick photoresist followed by attaching the topside to a transient substrate serving as a mechanical support carrier during Si removal. Then, the Si is thinned down to 100 μm thickness using chemical-mechanical lapping followed by dry etching by xenon difluoride (XeF_2) to remove the residual Si. After reaching the stop layer (AlN), the processed Si side is bought into contact with 3M sticky tape and washed with acetone to dissolve the photoresist and release the device from the transient substrate. Outstanding sheet resistance, high mobility, and sheet carrier density were reported to be 437Ω, 1831 cm^2/V.s, and 9×10^{12} cm^{-2}, respectively. In

addition, a high I_{ON} /I_{OFF} ratio (10^5) and a maximum current density of 620 mA/mm, and high transconductance were observed at V_{GS} = -2.2 V and a pinch-off value of -3.3 V with a value of 239 mS/mm. To assure the feasibility of using 3M flexible tape in integrated circuits, Mhedhbi *et al.* also used the flexible tape as the carrier for a coplanar propagation waveguide (CPW). The imperative parameters to evaluate the CPW performance over a frequency range (0-60 GHz) indicate low attenuation up to as 0.2 dB/mm at 10 GHz for a 1 mm length CPW, which is in good agreement with a similar CPW on undoped rigid Si (111). [67]

For harsh-environment materials that are grown on a rigid substrate, the quality of the released thin film is crucial to the device function. Eliminating the defect density in a material intended to fulfill the requirements of harsh-environment operating conditions results in better material stability. [68–70] Several studies have been carried out to improve material quality by terminating the introduced defect originating during epitaxial crystal growth as a result of lattice mismatch or thermal expansion coefficient mismatch. [71–73]

Cheng *et al*. investigated variable compositions of SiC as a buffer layer to grow GaN on thermal-oxidized Si substrate fabricated GaN-based high-power LEDs, followed by immersion into a buffer oxide etching (BOE) solution to etch the SiO_2 buffer to produce a flexible GaN configuration. The flexible GaN-based LEDs obtained after the transfer process can be observed in Figure 4a. The study shows that C-rich SiC composition deposited using low-temperature plasma enhanced chemical vapor deposition allows strain relaxation, which suppresses interfacial defects and explains the superiority of LEDs on C-rich SiC as a buffer layer compared with a Si-rich SiC buffer layer. [70]

3.1.2. Epitaxial Lift-off (ELO)

Achieving flexibility in material platforms for harsh environments is a significant challenge

especially if the material is chemically resistant, which makes the etching process difficult. GaN is a widely studied harsh-environment material for inducing flexible devices. The bandgap-selective epitaxial lift-off (ELO) process of GaN is a promising method to separate thin GaN layers from a foreign or native substrate after crystal growth. The ELO process demonstrated by Youtsey *et al.* relies on targeting the InGaN sacrificial layer using selective photo-enhanced wet etching. To facilitate the entire separation, the backside of the substrate is UV illuminated with energy below the bandgap of the substrate material, which works with the KOH solution to etch the remaining InGaN. The UV illumination generates electron-hole pairs in the semiconductor material as the photogenerated holes yield to the oxidation of the InGaN, which causes dissolution, whereas an external cathode is used to collect the photogenerated electrons. Finally, the floating GaN layer is bonded to the carrier of interest followed by metal-layer removal. The ELO process flow is depicted in Figure 4b and a lifted-off ELO foil from the GaN substrate can be observed in Figure 4c. [37]

The ELO process drastically reduces costs as the host substrate is reusable and can grow thin films multiple times, in addition to the non-destructive behavior of the ELO process during separation. The ELO process provides high yield in comparison with the Laser lift-off process. Besides that, it is applicable to both foreign and native substrates, unlike Laser lift-off. More importantly, this process is compatible with growing the entire stack using MOCVD including the sacrificial layer, which leads to high-quality, freestanding GaN layers. [37]

3.1.3. Direct Fabrication on the Flexible Substrate

Fabricating flexible electronic systems directly on flexible carriers has been hindered by manufacturing incompatibility in terms of using high temperature during deposition and annealing or aggressive chemical during wet/dry etching. [74,75] Controlling the thermal budget of

the fabrication process enables the direct realizing of devices on flexible substrates.[76] Direct device fabrication on flexible substrates offers high throughput in contrast to the conventional transferring method. Bolat *et al.* presented a GaN-based thin film transistor directly fabricated on a flexible polyethylene naphthalate (PEN) substrate with a thermal budget below 200 °C. [77] The bottom gated TFTs with GaN channels were fabricated on a rigid substrate (highly doped p-type Si wafer) and on a flexible polyethylene naphthalate (PEN) substrate to compare the electrical performance and stability under gate bias stress. It was observed that critical device parameters including the I_{ON}/I_{OFF} current ratio, threshold voltage, and carrier mobility varied significantly between rigid and flexible substrates. The I_{ON}/I_{OFF} current ratio dropped from 2×10^3 for rigid substrates to 7×10^2 for flexible ones. The obtained mobility is low for rigid and flexible substrates up to 0.005 cm^2/V.s and 0.0012 cm^2/V.s, respectively. The low mobility stems from the defects and nanocrystalline features of the GaN thin film deposited by atomic layer deposition (ALD). The threshold voltage of TFT on Si reaches 0.25 V, whereas it reaches 2.5 V on the flexible (PEN) substrate. The variation in threshold voltage was related to the higher O_2 concentration in the deposited GaN on the flexible (PEN) substrate. Optimizing the thin film properties to reduce the charge trap states at the insulator/semiconductor interface will result in comparable performance to TFT on the rigid substrate. The small threshold voltage alteration up to 0.14V in the threshold voltage shift of high-performance ZnO-based TFT under the same stress conditions suggests the extraordinarily stable characteristics of TFT on the flexible substrate. [77]

Direct fabrication on a flexible substrate also poses a great challenge of handling the substrate. While rigid substrates and devices can be easily handled without much of care, extreme care needs to be given in handling flexible substrate due to their fragility and in case of

polymeric substrates due to their ability to hold static charges which can easily cause wrinkles in the substrate causing defects. Moreover, polymeric and elastomeric flexible substrates are also not suitable for standard state-of-the-art technologies thereby restricting the manufactural scale applications. Thus, the idea of volumetric reduction of the existing electronic devices using different techniques followed by flexible packaging and encapsulation for providing mechanical stability and reliability promises the pragmatic approach as has been discussed in this review article later. [10,65,78–80]

3.2. Design and Architecture for Stretchable Devices

Stretchable electronics are attracting increasing attention similar to what flexible electronics previously attracted due to exciting applications where nonplanar and non-uniform surfaces and complex host geometries are involved. Stretchability in any material or device introduces the ability to comply with arbitrary 3D surface curvature and usability over a wide range of sizes. Stretchability enables device deformability, which important in particular fields, such as biomedical, textile electronics, robots, and 3D displays. Stretchable platforms provide a unique benefit of an extra degree of freedom in design beyond flexibility and foldability that are traditionally limited to 2D curved surfaces. These properties make it widely popular for applications in wearable and biomedical electronics. [81–83]The choice of material and design of stretchable electronics for harsh environments must be dependent on the function and correlated to the environment as well complying with repeated tensile stress and hostile factors to ensure maintaining reliable peak performance under unusual circumstances.

A unique design is one way to obtain stretchable configurations. Tompkins *et al.* adopted a stress relief design (‘waves’) to achieve a stretchable AlGaN/GaN HEMT to withstand 10 % strain. They studied the effects of several design control parameters involving the angle between

the gate and the source-drain contacts, the variation of the gate length and the gate position along the sinusoid on electrical device performance. The dominant operation of HEMT in the saturation regime makes it possible for this structure to be used efficiently in stretchable configurations. However, it adversely affected the threshold voltage and transconductance. An increased shift in the threshold voltage was observed with different increasing contact angles. Additionally, investigations on the relationship between the gate length and the saturation current, I_{sa}, revealed that increasing the gate length meant more pronounced stress effects under curved configurations and implied less saturation current in contrast to the short gate, which behaves like a fairly straight gate due at the same radius of curvature. [84]

The decades-old art of Origami and Kirigami remain an attraction for many decades which lays the foundation of modern stretchable material design and applications. The material can be converted into flexible or stretchable entirely based on the geometrical or modular transformation.[85–89] In the recent past, Zhou et al. have transformed rigid carbon paper into a flexible and stretchable substrate platform by adopting a unique design technique of folding carbon paper in different angles. This foldable carbon (FC) paper was successfully demonstrated to be used as a functional material for self-charging power supply. The foldable design helped in achieving stable performance under different mechanical deformation such as rolling, twisting, and bending. The self-charging power supply system uses FC paper-based triboelectric nanogenerator (FC-TENG) and FC based supercapacitors (FC-SC) for storing the generated power. Adjusting the folding angle of carbon paper in triangle folding configuration help in tuning experienced tensile strain. The capability of the power system to maintain its function under mechanical deformation along with the waterproof feature of packaging material enhance its utility in a harsh environment which imposes continues deformation such as wearable

devices.[90]

The crucial role of intelligent design can be understood more aptly in the context of energy-harvesting devices deployed in harsh environments. Harvesting mechanical and thermal energy, which undergoes severe fluctuation, requires careful selection of active materials and robust design to withstand the extreme operating conditions. For example, Ko *et al* successfully demonstrated a hybrid piezoelectric-pyroelectric lead zirconium titanate (PZT)-based nanogenerator that can operate perfectly at 100 °C under harsh environment conditions involving extreme humidity up to 70% and aggressive base medium pH (=13). The structure of (PZT)-based nanogenerator consists of Ni−Cr metal foil coated with a $LaNiO_3$(LNO) bottom electrode. The bottom electrode has a perovskite structure, which facilities the uniform nucleation sites for PZT. The last two layers in the device structure include 2-µm-thick PZT thin film and a circular-patterned top electrode (Pt). The flexible PZT thin film (thickness ~ 2 µm) is a suitable choice of material for energy harvesting due to the high piezoelectric coefficient (140 pC/N), high pyroelectric coefficient (50 nC/cm^2K), and high remanent electric polarization (28 $\mu C/cm^2$). The properties as mentioned earlier enable the PZT-based nanogenerator to scavenge the mechanical/ thermal energy from a variety of surrounding sources such as the human body and wind. The utility of PZT-based nanogenerator under a hostile condition is proven upon its operating at the exhaust pipe of a car where thermal and mechanical energy is successfully harvested from the hot, impulsive CO and CO_2 gases. A study of temperature effects on piezoelectric and pyroelectric coefficients revealed that the pyroelectric coefficient is directly proportional to temperature whereas the piezoelectric coefficient is inversely proportional to temperature. Neither the piezoelectric coefficient nor the pyroelectric coefficient ceases to exist at high temperatures up to 200 °C, suggesting the feasibility of using flexible PZT Nanogenerator at high

temperature. To further increase the output of NG, the piezoelectricity and pyroelectricity of PZT is exploited simultaneously through successive bending and unbending associated with cooling and heating in a synergistic manner Figure 5 a-c. It is found that the cooling process enhances the electric polarization of the PZT thin film owing to suppression of the thermal fluctuation in contrast to heating. The impact of the wind temperature and the wind speed on the short-circuit current density (Jsc) and on the surface charge density are reproduced in Figure 5 d-g, showing clearly that the higher surface charge density obtained at higher temperature difference. Moreover, the biomechanical energy from a human arm is harvested adequately (crook, wrist, and finger), suggesting that the highest output obtained upon bending and unbending motion of the crook of a human arm in compared with wrist and finger motion. [91]

Similarly, Zhong *et al.* successfully demonstrated a mechanical energy harvester suitable for harsh environments with outstanding performance and a much simpler fabrication process. [64] The device was characterized for temperatures up to 70 °C and high moisture levels without any noticeable degradation in the device performance. In this work, a polyethylene terephthalate (PET) electret film was used as the active piezoelectric material combined with ethylene vinyl acetate copolymer (EVA) acting as the adhesive layer. The fabrication process follows the depicted sequences in Figure (6-a). PET/EVA/PET laminated film possesses strong mechanical bonding characteristics enabling the film to withstand up to 33 N/cm^2 of shearing force before detachment. The change in the dipole moments of the inner air bubble, which originated from a corona charging method by applying frequent mechanical force, converts the electrostatic induction intensity to alternating electricity. The mechanical force applied by a human hand succeeded in generating ~ 0.444mW. Applying a mechanical stimulus leads to decreasing and increasing in the thickness of layer 2, which in turn causes compression and rarefaction in the air

bubble. This oscillating mechanical mechanism alters the dipole moments, generating fluctuations in the electrical potential between the two electrodes. Important progress was recorded in the maximum load peak power density, ~ 25.923 μW/cm^2, corresponding to load a peak current density of ~ 0.241 μA/cm^2 Figure (6-b). The load peak current density and associated transferred charge density is reported under sweeping the pressure, frequency, stimulated cycles in Figures 6(c-e).

Acute humidity is an environmental factor that can affect the electrical output of many generators. The proper selection of material and design allows stable output signals under high humidity. A flexible PET/EVA-based piezoelectric generator sustains its peak performance upon subjected to environmental stress under high moisture. [64]

Xu *et al.* presented an aero-elastic flutter-based triboelectric nanogenerator (AF-TENG) consisting of a sandwich structure with two layers of copper (100 nm thick) surrounding a membrane inside a cuboid acrylic channel. This provided invariable electrical characteristics regardless of the ambient humidity. The fluctuating in membrane motion is not changed by the humidity. Therefore, the frequency is selected to track the wind speed rather than the current and voltage output, giving AF-TENG the advantage of working in extreme humidity. [92]

Producing a device that is capable of withstanding hostile environments without sacrificing the targeted application requirements, such as transparency, flexibility, cost-effectiveness, and restricted operating voltage is challenging. One such example is a flexible and transparent heater that is capable to function properly in a harsh environment which introduced by Li *et al.* [93] The transparent heater is made of a Cu wire/alumina/polyimide composite, which satisfies the requirement of a high-performance transparent heater due to the low sheet resistance (RS) and the high optical transmittance (TR). The Cu wire/alumina/polyimide composite offers

antioxidation capability, atomic diffusion resistance, durability under mechanical deformation, and thermal stability. The final protective layer on top is a 60-nm-thick polyimide (PI) with a low thermal expansion coefficient, high glass transition temperature exceeding 350 °C, desirable mechanical properties, and high transparency. The heater's material (Cu wire/Al_2O_3/PI) exhibits low sheet resistance up to 8 Ωsq^2 and 91.4% transparency to visible light. The transparency of (Cu wire/Al_2O_3/PI) depends on the density of the Cu wires, which is determined based on the electrospinning time. The temperature-time profiles indicate that Cu wire/Al_2O_3/PI-based heater is capable of working to the best of its function for over 30 min and approaching the maximum temperature of 288 °C with a response time of 60 s when powered with 10 V (Fig 7a). Higher applied operating voltage (>10V) results in Cu wire fracture.

Investigations of the electric stability of the heater composite (Cu wire/Al_2O_3/PI) with different Al_2O_3 thicknesses and comparison with pure Cu wires with the Cu wire/PI demonstrated the importance of Al_2O_3 and determined the optimal thickness of the coating layer (Al_2O_3). The best film composite must withstand the highest current without temperature variation. Electromigration occurs in all three compared materials and composites, although the Cu wire/8nm-Al_2O_3/PI composite shows higher electrical current tolerance with the saturated temperature at 140 °C (Figure 7b).

Li *et al.* also reported high antioxidation stability of the heater operating under harsh conditions including high relative humidity up to 85% at 85 °C for 100 hours. This stability was ascribed to the Cu wire/Al_2O_3 network and the Cu wire/Al_2O_3/PI composite film. The antioxidation stability indicates the important role played by Al_2O_3 in isolating and withstanding harsh environments to protect the Cu wire from the surrounding oxygen and moisture. The Cu wire/Al_2O_3 network exhibits outstanding mechanical stability in comparison with ITO, a well-

known material for transparent flexible heaters when undergoing a tensile bending test with varying curvature radii from 100 to 2 mm. The electrical performance of the Cu wire/Al_2O_3/PI network remains stable even for the smallest curvature radii (2 mm) and no degradation was observed over 2000 cycles, whereas the ITO/PET heater showed obvious degradation upon reducing the curvature radius or increasing the bending cycles (Figure 7c-d). [93]

To summarize, the selection of right material for the right application with appropriate processing methods is the key defining factor in obtaining a reliable and stable device capable of withstanding defined harsh environments.

In the next section, we describe a few packaging techniques that can enhance the stability and improve the ability of traditional electronic devices and materials to withstand harsh environmental conditions.

4. PACKAGING FOR HARSH ENVIRONMENTS

In the flexible electronic devices intended for harsh environments, the packaging issue is as important as material selection and intelligent design. The packaging material provides effective protection, which in turn enhances the device lifetime. The packaging material should be selected considering: i) the device's material platform. ii) environmental stress, and iii) device function.[94–96]

The Device's Material Platform Matching between the packaging material and the device's material in terms of the thermal expansion coefficient is imperative to prevent any detachment or crack and will lead to reliable compact sealing. The packaging material must follow the mechanical properties closely to avoid a huge mechanical mismatch in the interface, thereby introducing stress-induced, unavoidable deformations and negatively influencing the performance. The packaging material must conform to the flexible and stretchable features of

structural materials to achieve the mechanical compliance of the entire system. [94–96]

Environmental stress the packaging material must have excellent stability in the hostile environment. In some cases, environmental stress tolerance of packaging material mitigates the need for the functional material to be resistant to harmful environmental factors, such as radiation, aggressive chemicals, and moisture, as it blocks these factors from reaching the functional material in space, marine, and wearable applications, respectively. [10] The material should act as an insulator that provides maximum isolation of the electronics from the harsh environment to reproduce reliable performance.

Device function It is of great importance that the packaging material protects the device without compromising the device performance. The packaging material's capability of efficient dissipation of generated heat is one way to maintain the peak performance of the device. [97] The packaging material criteria vary depending on the device function. For instance, transparency is critical in packaging material for a solar cell; this is not the case in wearable electronics. Similarly, for applications such as physical heating therapies, the heating element needs to be in contact with the body, even though electrical isolation needs to be present between the heating element and the body to avoid electrocution due to high currents flowing in the heating thermal patches.

Above all, the criteria for the packaging material for harsh environment applications depend on the kind of environmental stress and intended function. There cannot be one single versatile material that fits all purposes. Below, remarkable works on packaging materials for the harsh environment applications in space and marine environments are highlighted.

4.1. Packaging Materials for Space Applications

Flexible packaging of III–V-based solar cells for space applications is a challenging issue as

the space environment features several extreme conditions in terms of temperature, radiation, and pressure.[98]The packaging material must fulfill the requirements of transparency, reproducibility, radiation hardness, high vacuum stability, sufficient shielding capacity, minimum thickness, and lightweight. The radiation resistance property is of great importance when selecting solar cell packaging materials to avoid damage caused by high-energy UV that leads to material loss and generates chromophores that influence the transparency of polymer materials. Radiation resistance is also essential to provide protection against atomic oxygen (ATOX), encountered in low earth orbits, to avoid breaking organic bonds. The stability of the packaging material under high vacuum is also imperative as it suppresses the outgassing of volatile components that in turn can accumulate and contaminate other parts of the spaceship. Shielding capacity is another crucial factor that needs to be considered in the packaging material. It refers to the mass faced by the irradiated particles and is represented by the product of the material density and the layer thickness.

Different materials are synthesized and investigated based on the aforementioned criteria and the best candidate is doped with cerium (Ce) to boost its stability under vacuum conditions. The shielding capacity of the investigated material is adjusted to be comparable to that corresponding to the standard Ce-doped cover glass, CMX, which is used in the rigid panel configurations. Among the investigated materials (polyimide- polyhedral oligomeric silsesquioxanes POSS, tetraethoxysilane-polydimethylsiloxane TEOS-PDMS, and methyltrimethoxysilane-based siloxane (MBS)), MBS has the best properties in terms of simple synthesis, high reproducibility, and transparency, making it the optimal choice as a flexible shielding material for solar panels used on space ships. To synthesize MBS, methyltrimethoxysilane (MTMS) precursor is mixed with either tetramethylorthosilicate (TMOS), dimethyldimethoxysilane (DMDMS) or

phenyltrimethoxysilane (PhTMS) and heated to 100 °C in an oil bath followed by adding diluted HCl. Subsequently, the mixture is covered and stirred for 4–15 minutes. The MBS film exhibits high transmission, covering the wavelength range from 200 to 1250 nm. The transmission of MBS drops slightly after incorporation of Ce. [99]

4.2. Packaging for Marine Applications

In marine applications, having the optimal resilience to accommodate marine species movement and sustain the best performance under harsh deep-sea environments require careful consideration of functional materials and packaging materials. In addition, the materials must withstand high pressure and salinity. The material must be biocompatible, lightweight, and robust. Shaikh *et al.* designed a flexible marine skin consisting of a wireless multi-sensory platform that is capable of measuring the temperature, depth, pressure, and salinity with unique features such as being waterproof, lightweight (<2.4g), cost-effective, adaptability to tag a diverse set of underwater animals non-invasively without any discomfort. [10,78] The choice of the active material as well as for packaging plays a crucial role in developing such devices. The flexibility and the stretchable design of the entire device help to make it conformal with the animal body without affecting the natural movement of the animal and without compromising the multi-sensory platform's performance. Polydimethylsiloxane (PDMS)- one of the most widely used material in the flexible devices development research has been demonstrated by the group to be an excellent encapsulating material in marine applications owing to its biocompatibility, hydrophobicity, inherent flexibility and stretchability. The material properties of this soft-polymer are not altered significantly due to environmental factors such as salinity, temperature, and pressure once the polymer is cured. The active material for electrodes design is a low-cost electrochemical deposited (ECD) Cu providing stability and reliable performance at

higher depths inside the seawater. Although Cu is prone to corrosion, the encapsulation material helps in protecting the corrosion of Cu tested over extended periods of deployment underwater for up to 6 weeks at stretch.

To provide mechanical stability and reduce the stresses generated from material deformation, electrode materials are sandwiched between the soft-polymer on both sides that neutralizes the mismatch of the mechanical deformation stresses. The multisensory platform design consists of a wavy network patterned array of capacitive-based pressure sensors and a resistive-based temperature detector associated with a simple salinity sensor. The multisensory platform is then combined with an optimal interface system in terms of size and weight. The electrode material for this device was ECD Cu having a thickness of 5 µm deposited on a 10 µm thick Polyimide PI as a flexible substrate to provide mechanical strength and good adhesion. Complete fabrication and integration of the flexible marine skin system are shown in (Figure 8a).

The PI provides mechanical strength to the deposited metal layers to avoid any crack while stretching the entire structure. The dielectric of the pressure sensor is made of 50-µm-thick PDMS. The designed marine skin attached to the epidermal surface of a crab using biocompatible superglue to investigate its performance in an in-situ study (Figure 8b). The performance of the pressure sensor provides depth patterns and reveals real-time tracking of the crab's up/down water movement for 6 min. Results for temperature, depth, and salinity were compared with commercially available bulky products for marine environmental monitoring.[10] The performance of the marine skin is reported to be on par with the commercial devices. The flexible and stretchable devices and the packaging for adaptability with the harsh environment make a clear case for the future unprecedented applications.

5. CONCLUSION AND OUTLOOK

Electronics that dominate the large portion of day-to-day human activities revolve around semiconductor devices. The miniaturization and the state-of-the-art CMOS technology drove the development of electronics to devices ranging from smaller than a hair diameter (< 150 um) to as large as the giant airplanes and satellites. Silicon has been the main ingredient in more than 90% of these electronic devices. The curiosity to understand nature and life and to explore the universe has driven unanticipated scientific discoveries and thereby had led to advances in electronics in areas unimaginable a few decades ago. The applications in space missions, satellites, underwater exploration, wearables, oil and gas industries, and nuclear reactors and power generation form a non-exhaustive list of harsh environments. The behavior of silicon to varying harsh conditions specifically at elevated temperatures has generated an interest in the development of new materials and innovative design strategies for such applications.

We have presented throughout this paper that harsh environments do not adhere to a single definition. Harsh environments are any environment that deviates and degrades the normal performance of the electronic device. We have presented how important it is to choose the correct material for a specific application based on the environmental conditions. We described general criteria that can be followed in choosing a correct material candidate for harsh environments. In electronics, the most fundamental building block is a transistor and mainly CMOS-based processes are used for fabrication of these devices from silicon semiconducting materials. However, the materials for harsh environments can vary drastically in properties compared to silicon and hence the process of fabrication can vary. Flexible electronics have attracted huge attention due to their promising applications and capability to conform with complex architectures and living bodies. Progress in the development of flexible electronics has

led to many processes that achieve flexibility in rigid silicon-based devices. They include trench protect etch release, soft etch back, corrugation, SOI, spalling and many other transfer techniques for inorganic devices. In addition, a lot of effort has been expended on organic devices to obtain flexible devices for large-area applications using low-end fabrication techniques.

Similarly, to comply with the existing CMOS technologies, there is a need to address and come up with novel ideas for obtaining flexible electronic devices for harsh environments. In addition to the flexibility, stretchability of these devices has attracted significant interest in the scientific community due to its advantages for use in a wide variety of application areas. Rogers' group has been actively involved in obtaining stretchable devices using fractal design concepts. [22,30]Recently, Hussain's group has demonstrated remarkable progress in producing flexible and stretchable electronic devices using standard CMOS technologies, including stretchable silicon fabric, stretchable thermal patches, stretchable antennas, fully spherical stretchable photodetector arrays, Marine Skin. They also studied the mechanics of the stretchability. [10,11,23,33–35,100–102]

We believe that applying unconventional techniques to the materials for harsh environments and capitalizing on recent advances from stretchable and flexible silicon-based devices can lead to a disruption in the electronics for the harsh environments.

References:

[1] P. G. Neudeck, R. S. Okojie, L. Y. Chen, *Proc. IEEE* **2002**, *90*, 1065.

[2] R. Bogue, *Sens. Rev.* **2002**, *22*, 113.

[3] A. P. (Berkeley S. and A. C. Pisano, **2013**.

[4] J. Yang, T. Caillat, *MRS Bull.* **2006**, *31*, 224.

[5] A. I. Kalina, *Dual Pressure Geothermal System*, **2004**.

[6] M. P. Durisic, Z. Tafa, G. Dimic, V. Milutinovic, *Mediterr. Conf. Embed. Comput.* **2012**, 196.

[7] S. V. Garimella, A. S. Fleischer, J. Y. Murthy, A. Keshavarzi, R. Prasher, C. Patel, S. H. Bhavnani, R. Venkatasubramanian, R. Mahajan, Y. Joshi, B. Sammakia, B. A. Myers, L. Chorosinski, M. Baelmans, P. Sathyamurthy, P. E. Raad, *IEEE Trans. Components Packag. Technol.* **2008**, *31*, 801.

[8] E. Zakar, *Proc. Army Sci. Conf.* **2004**, 1.

[9] A. Mohan, A. P. Malshe, S. Aravamudhan, S. Bhansali, in *Electron. Components Technol. Conf. 2004. Proceedings. 54th*, IEEE, **2004**, pp. 948–950.

[10] J. M. Nassar, S. M. Khan, S. J. Velling, A. Diaz-Gaxiola, S. F. Shaikh, N. R. Geraldi, G. A. Torres Sevilla, C. M. Duarte, M. M. Hussain, *npj Flex. Electron.* **2018**, *2*, 13.

[11] A. M. Hussain, F. A. Ghaffar, S. I. Park, J. A. Rogers, A. Shamim, M. M. Hussain, *Adv. Funct. Mater.* **2015**, *25*, 6565.

[12] R. E. Smallman, R. J. Bishop, in *Met. Mater.*, Wiley, Hoboken, NJ, **1995**, pp. 87–129.

[13] L. Ratke, in *Util. Sp. Today Tomorrow*, John Wiley & Sons, Inc, New York, **2006**, pp. 297–340.

[14] V. Sudarsan, in *Mater. Under Extrem. Cond. Recent Trends Futur. Prospect.* (Eds.: A.K.

Tyagi, S. Banerjee), Elsevier, Amsterdam, **2017**, pp. 129–158.

[15] W. S. Tait, *Handbook of Environmental Degradation of Materials*, William Andrew /Elsevier, Oxford, **2005**.

[16] Y. D. Kim, H. Kim, Y. Cho, J. H. Ryoo, C.-H. Park, P. Kim, Y. S. Kim, S. Lee, Y. Li, S.-N. Park, Y. S. Yoo, D. Yoon, V. E. Dorgan, E. Pop, T. F. Heinz, J. Hone, S.-H. Chun, H. Cheong, S. W. Lee, M.-H. Bae, Y. D. Park, *Nat. Nanotechnol.* **2015**, *10*, 1.

[17] R. Raccichini, A. Varzi, S. Passerini, B. Scrosati, *Nat. Mater.* **2015**, *14*, 271.

[18] Y. D. Kim, Y. Gao, R. J. Shiue, L. Wang, O. B. Aslan, M. H. Bae, H. Kim, D. Seo, H. J. Choi, S. H. Kim, A. Nemilentsau, T. Low, C. Tan, D. K. Efetov, T. Taniguchi, K. Watanabe, K. L. Shepard, T. F. Heinz, D. Englund, J. Hone, *Nano Lett.* **2018**, *18*, 934.

[19] M. S. Cao, X. X. Wang, W. Q. Cao, J. Yuan, *J. Mater. Chem. C* **2015**, *3*, 6589.

[20] J. Watson, G. Castro, *Analog Dialogue* **2012**, *46*, 1.

[21] P. S., V. M., B. Z. A, *Nanoscale* **2013**, *5*, 1727.

[22] J. A. Rogers, A. J. Baca, J. Ahn, Y. Sun, M. A. Meitl, E. Menard, H.-S. Kim, W. M. Choi, D. Kim, Y. Huang, *Angew. Chemie Int. Ed.* **2008**, *47*, 5524.

[23] G. A. Torres Sevilla, M. T. Ghoneim, H. Fahad, J. P. Rojas, A. M. Hussain, M. M. Hussain, *ACS Nano* **2014**, *8*, 9850.

[24] R. R. Bahabry, A. T. Kutbee, S. M. Khan, A. C. Sepulveda, I. Wicaksono, M. Nour, N. Wehbe, A. S. Almislem, M. T. Ghoneim, G. A. Torres Sevilla, A. Syed, S. F. Shaikh, M. M. Hussain, *Adv. Energy Mater.* **2018**, *8*, DOI 10.1002/aenm.201702221.

[25] S. J. Kim, H. E. Lee, H. Choi, Y. Kim, J. H. We, J. S. Shin, K. J. Lee, B. J. Cho, *ACS Nano* **2016**, *10*, 10851.

[26] S. F. Shaikh, M. T. Ghoneim, G. A. Torres Sevilla, J. M. Nassar, A. M. Hussain, M. M.

Hussain, *IEEE Trans. Electron Devices* **2017**, *64*, 1894.

[27] A. M. Hussain, S. F. Shaikh, M. M. Hussain, *AIP Adv.* **2016**, *6*, DOI 10.1063/1.4959193.

[28] J. Kang, D. Shin, S. Bae, B. H. Hong, *Nanoscale* **2012**, *4*, 5527.

[29] K. Zhang, J. H. Seo, W. Zhou, Z. Ma, *J. Phys. D. Appl. Phys.* **2012**, *45*, 143001.

[30] D.-H. Kim, R. Ghaffari, N. Lu, J. A. Rogers, *Annu. Rev. Biomed. Eng.* **2012**, *14*, 113.

[31] H. Keum, A. Carlson, H. Ning, A. Mihi, J. D. Eisenhaure, P. V Braun, J. A. Rogers, S. Kim, *J. Micromechanics Microengineering* **2012**, *22*, 55018.

[32] H. Keum, H. J. Chung, S. Kim, *ACS Appl. Mater. Interfaces* **2013**, *5*, 6061.

[33] M. Hussain, J. P. Rojas, G. A. Torres Sevilla, *SPIE Newsrooms* **2013**, DOI 10.1117/2.1201311.004863.

[34] J. P. Rojas, G. A. Torres Sevilla, N. Alfaraj, M. T. Ghoneim, A. T. Kutbee, A. Sridharan, M. M. Hussain, *ACS Nano* **2015**, *9*, 5255.

[35] J. P. Rojas, G. A. Torres Sevilla, M. T. Ghoneim, S. Bin Inayat, S. M. Ahmed, A. M. Hussain, M. M. Hussain, *ACS Nano* **2014**, *8*, 1468.

[36] S. H. Kim, S. Singh, S. K. Oh, D. K. Lee, K. H. Lee, S. Shervin, M. Asadirad, V. Venkateswaran, K. Olenick, J. A. Olenick, S. N. Lee, J. S. Kwak, A. Mavrokefalos, J. H. Ryou, *IEEE Electron Device Lett.* **2016**, *37*, 615.

[37] C. Youtsey, R. McCarthy, R. Reddy, K. Forghani, A. Xie, E. Beam, J. Wang, P. Fay, T. Ciarkowski, E. Carlson, L. Guido, *Phys. Status Solidi Basic Res.* **2017**, *254*, DOI 10.1002/pssb.201600774.

[38] P. Wang, L. Cheng, Y. Zhang, H. Wu, Y. Hou, W. Yuan, L. Zheng, *Ceram. Int.* **2017**, *43*, 7424.

[39] S. Chen, M. Shang, F. Gao, L. Wang, P. Ying, W. Yang, X. Fang, *Adv. Sci.* **2016**, *3*,

1500256.

[40] R. Wu, K. Zhou, C. Y. Yue, J. Wei, Y. Pan, *Prog. Mater. Sci.* **2015**, *72*, 1.

[41] C. H. Voon, B. Y. Lim, L. N. Ho, in *Synth. Inorg. Nanomater.*, Elsevier, **2018**, pp. 213–253.

[42] B. Sun, Y. Sun, C. Wang, *Small* **2018**, *14*, 1703391.

[43] L. Zhang, M. N. Fairchild, S. D. Hersee, P. Varangis, A. K. Rishinaramangalam, *J. Mater. Res.* **2011**, *26*, 2293.

[44] S. D. Hersee, X. Sun, X. Wang, *Nano Lett.* **2006**, *6*, 1808.

[45] R. Rakesh Kumar, K. Narasimha Rao, A. R. Phani, *Appl. Nanosci.* **2011**, *1*, 211.

[46] B. J. May, A. T. M. G. Sarwar, R. C. Myers, *Appl. Phys. Lett.* **2016**, *108*, 141103.

[47] G. Calabrese, P. Corfdir, G. Gao, C. Pfüller, A. Trampert, O. Brandt, L. Geelhaar, S. Fernández-Garrido, *Appl. Phys. Lett.* **2017**, *111*, 219901.

[48] C. Dames, et al., *ChemInform* **2016**, *47*, 4684.

[49] M. Han, X. Yin, Z. Hou, C. Song, X. Li, L. Zhang, L. Cheng, *ACS Appl. Mater. Interfaces* **2017**, *9*, 11803.

[50] P. Li, J. G. Ma, H. Y. Xu, H. C. Zhu, Y. C. Liu, *Appl. Phys. Lett.* **2017**, *110*, 161901.

[51] S. Bose, in *High Temp. Coatings*, Butterworth-Heinemann, **2018**, pp. 45–72.

[52] V. Nam, D. Lee, *Nanomaterials* **2016**, *6*, 47.

[53] D. Kim, J. Kwon, J. Jung, K. Kim, H. Lee, J. Yeo, S. Hong, S. Han, S. H. Ko, *Small Methods* **2018**, *2*, 1800036.

[54] L. Shi, R. Wang, H. Zhai, Y. Liu, L. Gao, J. Sun, *Phys. Chem. Chem. Phys.* **2015**, *17*, 4231.

[55] R. Pflumm, S. Friedle, M. Schütze, *Intermetallics* **2014**, *56*, 1.

[56] M. Seifert, G. K. Rane, S. B. Menzel, S. Oswald, T. Gemming, *J. Alloys Compd.* **2019**, *776*, 819.

[57] T. Ikeda, K. Shiba, *Mater. Trans.* **2016**, *57*, 860.

[58] K. S. Kim, J. Y. Song, E. K. Chung, J. K. Park, S. H. Hong, in *Mech. Mater.*, Elsevier, **2006**, pp. 119–127.

[59] Z. W. Zhong, *Microelectron. Int.* **2009**, *26*, 10.

[60] E. Brachmann, M. Seifert, D. Ernst, S. B. Menzel, T. Gemming, *Sensors Actuators, A Phys.* **2018**, *284*, 129.

[61] W. Park, J.-W. Min, S. F. Shaikh, M. M. Hussain, *Phys. Status Solidi Appl. Mater. Sci.* **2017**, *214*, DOI 10.1002/pssa.201700534.

[62] W. Park, S. F. Shaikh, J.-W. Min, S. K. Lee, B. H. Lee, M. M. Hussain, *Nanotechnology* **2018**, *29*, DOI 10.1088/1361-6528/aac4b9.

[63] A. Buchberger, S. Peterka, A. M. Coclite, A. Bergmann, *Sensors (Basel).* **2019**, *19*, 999.

[64] J. Zhong, Q. Zhong, X. Zang, N. Wu, W. Li, Y. Chu, L. Lin, *Nano Energy* **2017**, *37*, 268.

[65] S. F. Shaikh, M. T. Ghoneim, R. R. Bahabry, S. M. Khan, M. M. Hussain, *Adv. Mater. Technol.* **2018**, *3*, 1700147.

[66] M. M. Hussain, Z. (Jack) Ma, S. F. Shaikh, *Electrochem. Soc. Interface* **2018**, *27*, 65.

[67] S. Mhedhbi, M. Lesecq, P. Altuntas, N. Defrance, E. Okada, Y. Cordier, B. Damilano, G. Tabares-Jimenez, A. Ebongue, V. Hoel, *IEEE Electron Device Lett.* **2016**, *37*, 553.

[68] L. Schmidt-Mende, J. L. MacManus-Driscoll, *Mater. Today* **2007**, *10*, 40.

[69] P. Makaram, J. Joh, J. A. Alamo, T. Palacios, C. V Thompson, P. Makaram, J. Joh, J. A. Alamo, T. Palacios, *Appl. Phys. Lett.* **2014**, *233509*, 2012.

[70] C.-H. Cheng, A.-J. Tzou, J.-H. Chang, Y.-C. Chi, Y.-H. Lin, M.-H. Shih, C.-K. Lee, C.-I.

Wu, H.-C. Kuo, C.-Y. Chang, G.-R. Lin, *Sci. Rep.* **2016**, *6*, 19757.

[71] C. H. Cheng, T. W. Huang, C. L. Wu, M. K. Chen, C. H. Chu, Y. R. Wu, M. H. Shih, C. K. Lee, H. C. Kuo, D. P. Tsai, G. R. Lin, *J. Mater. Chem. C* **2017**, *5*, 607.

[72] S. Hu, S. Liu, Z. Zhang, H. Yan, Z. Gan, H. Fang, *J. Cryst. Growth* **2015**, *415*, 72.

[73] W. Wang, H. Wang, W. Yang, Y. Zhu, G. Li, *Sci. Rep.* **2016**, *6*, 24448.

[74] M. J. Madou, *Fundamentals of Microfabrication and Nanotechnology, Three-Volume Set*, CRC Press, Boca Raton, FL, **2018**.

[75] J. D. Plummer, M. D. Deal, P. B. Griffin, in *Silicon VLSI Technol.*, Prentice Hall, Upper Saddle River, NJ, **2000**, p. 32.

[76] A. Sazonov, D. Striakhilev, C. H. O. Lee, A. Nathan, *Proc. IEEE* **2005**, *93*, 1420.

[77] S. Bolat, Z. Sisman, A. K. Okyay, *Appl. Phys. Lett.* **2016**, *109*, 233504.

[78] S. F. Shaikh, H. F. Mazo-Mantilla, N. Qaiser, S. M. Khan, J. M. Nassar, N. R. Geraldi, C. M. Duarte, M. M. Hussain, *Small* **2019**, *15*, 1804385.

[79] M. M. Hussain, S. F. Shaikh, G. A. T. Sevilla, J. M. Nassar, A. M. Hussain, R. R. Bahabry, S. M. Khan, A. T. Kutbee, J. P. Rojas, M. T. Ghoneim, M. Cruz, in *2018 76th Device Res. Conf.*, IEEE, **2018**, pp. 1–2.

[80] S. M. Khan, N. Qaiser, S. F. Shaikh, L. J. Ding, M. M. Hussain, *Flex. Print. Electron.* **2019**, *4*, 025001.

[81] T. L??her, M. Seckel, A. Ostmann, in *Electron. Syst. Integr. Technol. Conf. ESTC 2010 - Proc.*, IEEE, **2010**, pp. 1–6.

[82] T. Löher, M. Seckel, R. Vieroth, C. Dils, C. Kallmayer, A. Ostmann, R. Aschenbrenner, H. Reichl, in *Proc. Electron. Packag. Technol. Conf. EPTC*, IEEE, **2009**, pp. 893–898.

[83] S. P. Lacour, J. Jones, S. Wagner, T. Li, Z. Suo, *Proc. IEEE* **2005**, *93*, 1459.

[84] R. P. Tompkins, I. Mahaboob, F. Shahedipour-Sandvik, N. Lazarus, *Solid. State. Electron.* **2017**, *136*, 36.

[85] J. A. Fan, W. H. Yeo, Y. Su, Y. Hattori, W. Lee, S. Y. Jung, Y. Zhang, Z. Liu, H. Cheng, L. Falgout, M. Bajema, T. Coleman, D. Gregoire, R. J. Larsen, Y. Huang, J. A. Rogers, *Nat. Commun.* **2014**, *5*, 1.

[86] N. Alcheikh, S. F. Shaikh, M. M. Hussain, *AIP Adv.* **2019**, *9*, DOI 10.1063/1.5053967.

[87] N. Alcheikh, S. F. Shaikh, M. M. Hussain, *Extrem. Mech. Lett.* **2018**, *24*, 6.

[88] N. Qaiser, S. M. Khan, M. Nour, M. U. Rehman, J. P. Rojas, M. M. Hussain, *Appl. Phys. Lett.* **2017**, *111*, DOI 10.1063/1.5007111.

[89] J. A. Rogers, T. Someya, Y. Huang, *Science (80-.).* **2010**, *327*, 1603.

[90] C. Zhou, Y. Yang, N. Sun, Z. Wen, P. Cheng, X. Xie, H. Shao, Q. Shen, X. Chen, Y. Liu, Z. L. Wang, X. Sun, *Nano Res.* **2018**, *11*, 4313.

[91] Y. J. Ko, D. Y. Kim, S. S. Won, C. W. Ahn, I. W. Kim, A. I. Kingon, S.-H. Kim, J.-H. Ko, J. H. Jung, *ACS Appl. Mater. Interfaces* **2016**, *8*, acsami.6b00054.

[92] M. Xu, Y. C. Wang, S. L. Zhang, W. Ding, J. Cheng, X. He, P. Zhang, Z. Wang, X. Pan, Z. L. Wang, *Extrem. Mech. Lett.* **2017**, *15*, 122.

[93] P. Li, J. Ma, H. Xu, X. Xue, Y. Liu, *J. Mater. Chem. C* **2016**, *4*, 3581.

[94] M. Gad-el-Hak, *MEMS: Design and Fabrication*, CRC/Taylor & Francis, Boca Raton, FL, **2006**.

[95] M. L. Locatelli, R. Khazaka, S. Diaham, C. D. Pham, M. Bechara, S. Dinculescu, P. Bidan, *IEEE Trans. Power Electron.* **2014**, *29*, 2281.

[96] C. Slater, R. Cojbasic, T. Maeder, Y. Leblebici, P. Ryser, *Addit. Conf. (Device Packag. HiTEC, HiTEN, CICMT)* **2015**, *2013*, 000184.

[97] Q. Zheng, Y. Jin, Z. Liu, H. Ouyang, H. Li, B. Shi, W. Jiang, H. Zhang, Z. Li, Z. L. Wang, *ACS Appl. Mater. Interfaces* **2016**, *8*, 26697.

[98] P. French, G. Krijnen, F. Roozeboom, *Microsystems Nanoeng.* **2016**, *2*, 16048.

[99] J. Feenstra, R. H. Van Leest, N. J. Smeenk, G. Oomen, E. Bongers, P. Mulder, E. Vlieg, J. J. Schermer, *J. Appl. Polym. Sci.* **2016**, *133*, DOI 10.1002/app.43661.

[100] A. T. Kutbee, R. R. Bahabry, K. O. Alamoudi, M. T. Ghoneim, M. D. Cordero, A. S. Almuslem, A. Gumus, E. M. Diallo, J. M. Nassar, A. M. Hussain, N. M. Khashab, M. M. Hussain, *npj Flex. Electron.* **2017**, *1*, 7.

[101] G. A. Torres Sevilla, A. S. Almuslem, A. Gumus, A. M. Hussain, M. E. Cruz, M. M. Hussain, *Appl. Phys. Lett.* **2016**, *108*, 0.

[102] J. M. Nassar, S. M. Khan, D. R. Villalva, M. M. Nour, A. S. Almuslem, M. M. Hussain, *npj Flex. Electron.* **2018**, *2*, 24.

[103] Y. J. Ko, D. Y. Kim, S. S. Won, C. W. Ahn, I. W. Kim, A. I. Kingon, S. H. Kim, J. H. Ko, J. H. Jung, *ACS Appl. Mater. Interfaces* **2016**, *8*, 6504.

TABLES

Table 1: Thermal tolerance of semiconductor materials and the maturity level of the fabrication process of devices. [2]

Material	Technological Maturity	Maximum Operating Temperature (°C)
Silicon	Very high	200 - 250
Silicon-on-insulator	Medium	250 - 300
Gallium arsenide	High	350 - 400
Gallium nitride	Very low	500+
Silicon carbide	Low	600 - 750+
Diamond	Very low	1000 - 1100

Table 2: Table 2: Environmental variables experienced in application areas

Application Area	Typical Temperature (°C)	Expected Pressure (MPa)	Corrosive Medium	Required Functionality	REF
Oil and Gas Exploration	275	10 – 40	Extreme stresses, aggressive chemicals	Pressure, temperature, hydrocarbon, strain sensing	[3]
Automotive Engines	300	10	Repeated thermal cycles, Extreme stresses	Pressure, temperature, flame speed, O_2 sensing, DC/AC inverter	[4]
Geothermal	375	2	Extreme stresses	Pressure, temperature, strain, H_2S	[5]

Industrial Gas Turbines	600	8	Combustion, Extreme stresses	Pressure, temperature, flame speed, acceleration	[3]
Aircraft Engines	600	100	Repeated thermal cycles, Extreme stresses	Pressure, temperature, flame speed,	[3]
Military Application	–55 to 150	Up to 689	Vibration, Contamination, Acceleration condition,	Wireless communication, Infrared imaging, Harmful material detectors (Nuclear, radiological, chemical)	[6–8]
Space Exploration	230 to 486	10	> 5 Mrad radiation exposure	Wireless communication	[7]
Marine Application	5 to 60	20	Salinity up to (35 - 40 PSU)	Temperature, Pressure, salinity sensing, wireless communication	[9,10]
Wearable Electronic	RT	Atmospheric pressure	Mechanical deformation like extreme bending, and stretching	Body vital signs sensing, Wireless communication	[11]

FIGURES

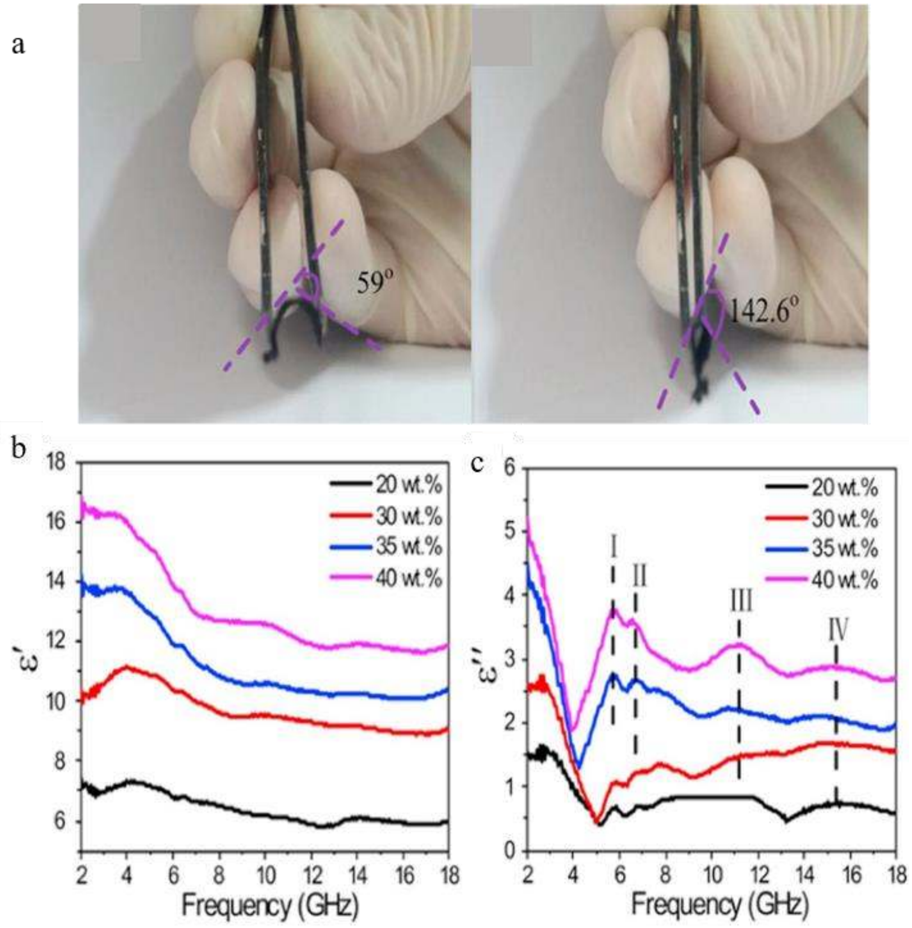

FIGURE 1: (a) Bending angle of flexible SiC ceramic nanofibers. Frequency dependence of (b) the real part, (c) imaginary part of the complex dielectric constant of a variable mass fraction of an SiC ceramic nanofiber. Reproduced (Adapted) with permission.[38] Copyright 2017, Ceramics International.

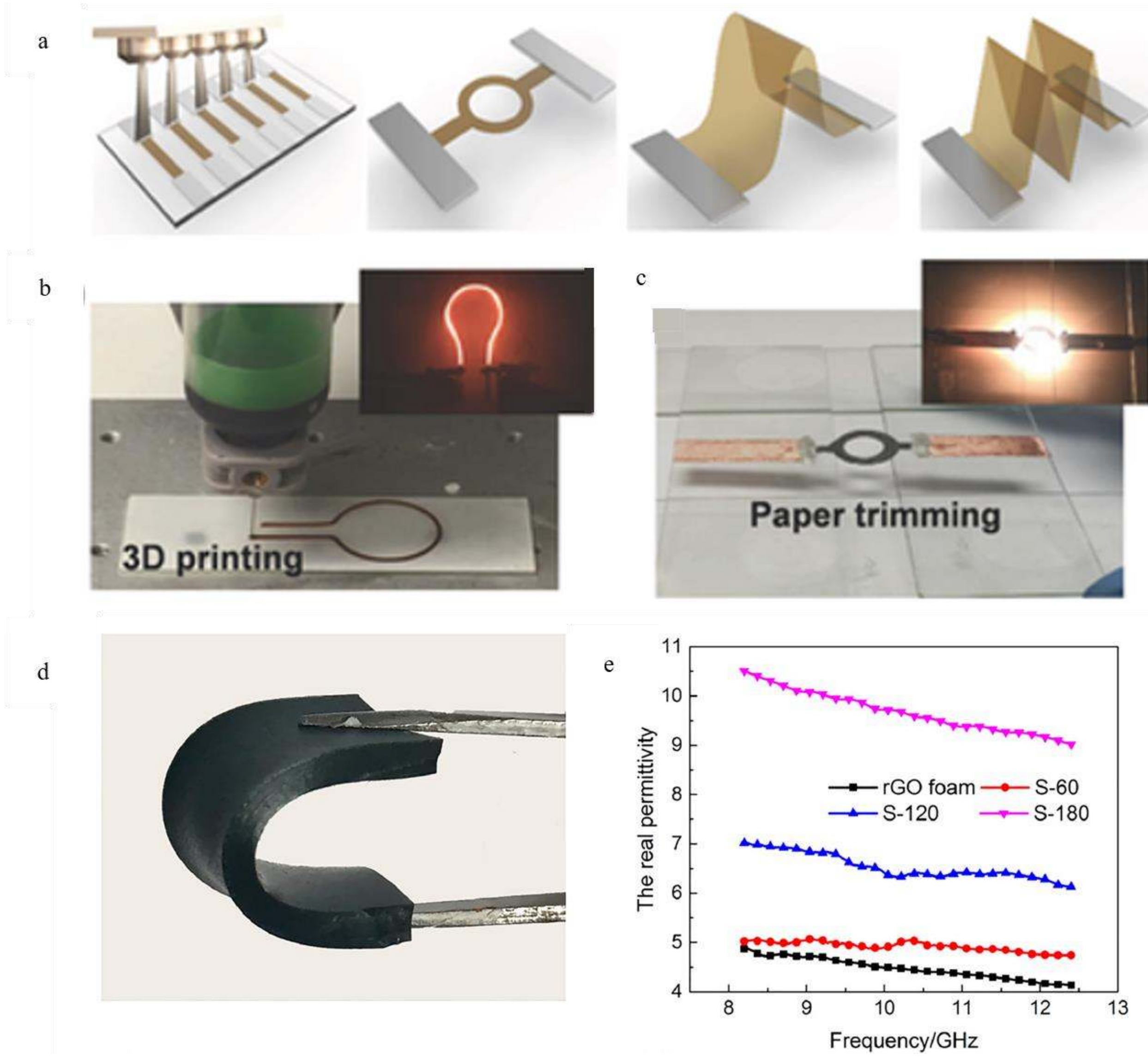

FIGURE 2: (a) The different configuration of flexible nanocarbon paper. (b) Nanocarbon-based light bulb fabricated using 3D printer. (c) Trimming nanocarbon paper into different shapes for illuminating. Reproduced (Adapted) with permission. [48] Copyright 2016, Advanced materials (d) Flexible rGO/SiC nanowires. (e) Frequency-dependent of the real part of permittivity of rGO, S-60, S-120, and S-180. Reproduced (Adapted) with permission. [49] Copyright 2017, ACS applied material & interfaces.

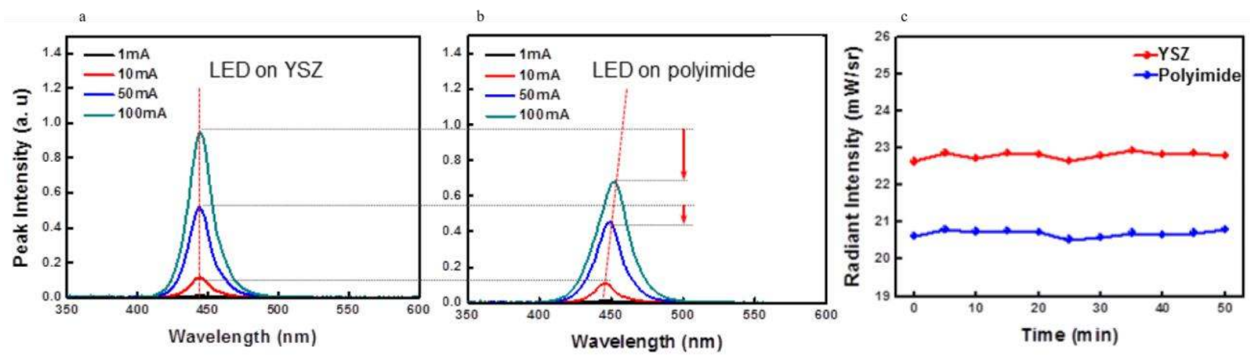

FIGURE 3: LED emission spectra on (a) YSZ substrate, (b) polyimide substrate for different injected current, and (c) LED output power vs. time at injected current of 100 mA on YSZ and polyimide substrates. Reproduced (Adapted) with permission. [36] Copyright 2016, Electron Device Letters.

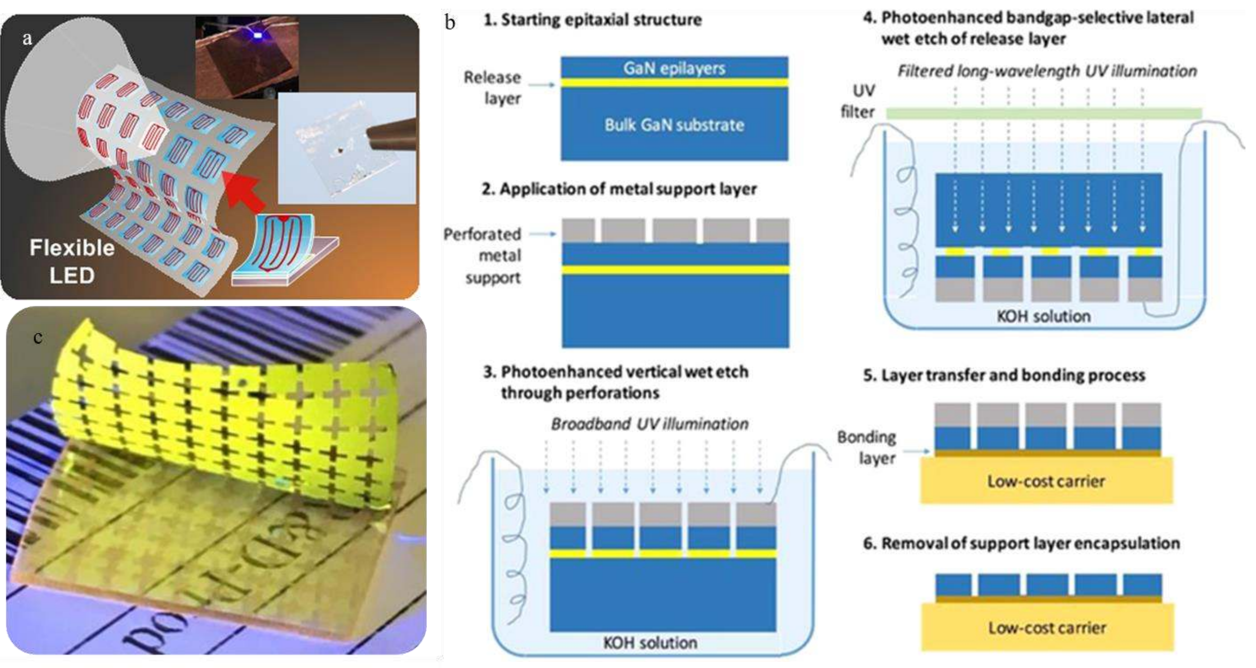

FIGURE 4: (a) GaN-based flexible LED. Reproduced (Adapted) with permission. [70] Copyright 2016, Scientific Reports. (b) Scheme of epitaxial lift-off process flow. (c) optical image of lifted-off ELO foil from GaN bulk substrate. Reproduced (Adapted) with permission. [37] Copyright 2017, Physica Status Solidi.

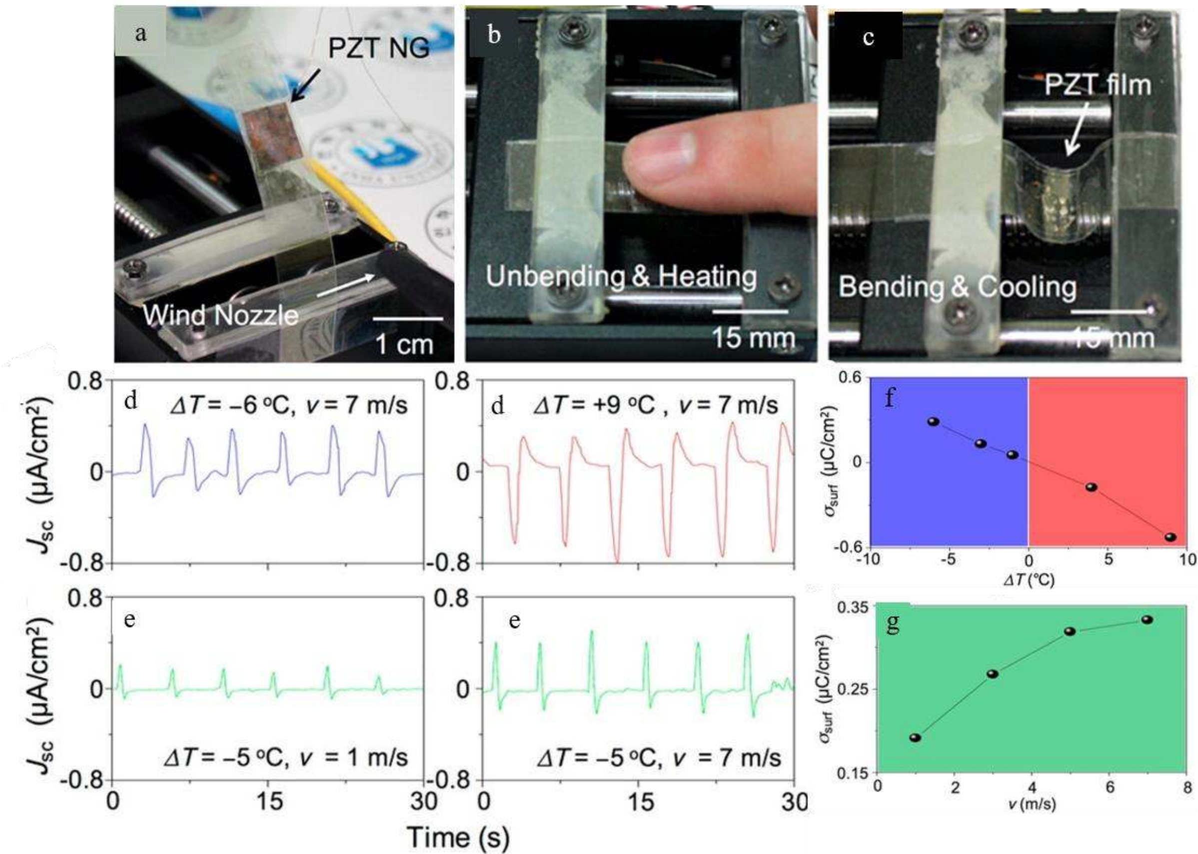

FIGURE 5: (a) Optical image of the experimental setup of mechanical / thermal energy harvesting in case of cold/hot winds. Optical image of the flexible PZT-based nanogenerator for (b) unbending and heating and (c) bending with cooling. Short-circuit current density, J_{sc}, as a function of (d) wind temperature at fixed speeds and (c) winds speed at fixed temperature variations. Surface charge density (σ_{surf}) as a function of (f) Temperature variation and (g) wind speed. Reproduced (Adapted) with permission. [103] Copyright 2016, ACS applied material & interfaces.

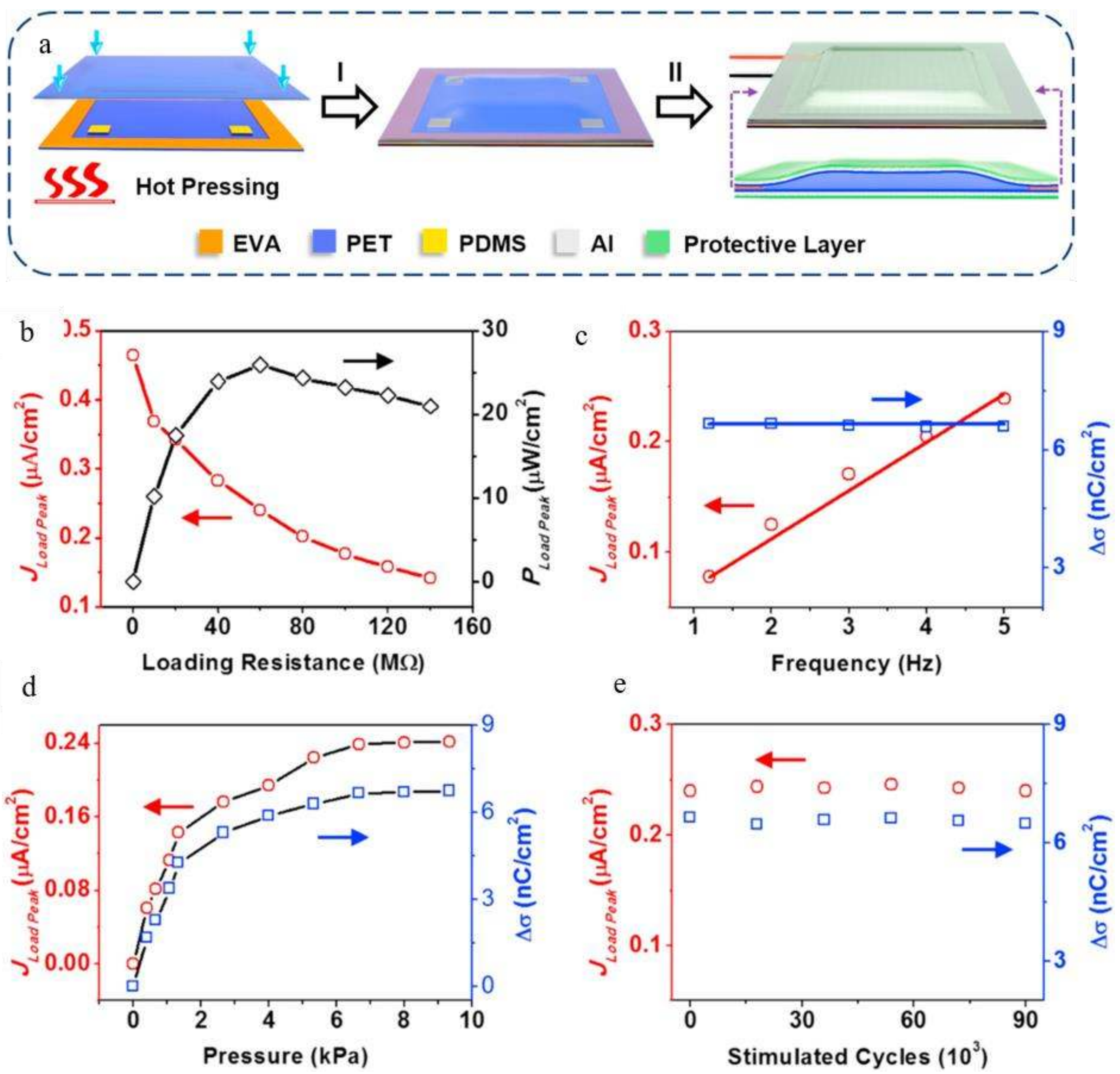

FIGURE 6: (a) Illustrative scheme of the fabrication flow of the flexible PET/EVA-based generator: (I) hot pressing and corona charging, (II) assembly of the electrode and protective layers. Electrical characteristic of the flexible PET/EVA-based piezoelectric generator. (b) Load peak current and power density of a generator vs. different load resistances, at P= $6.67X10^3$ Pa and f= 5 Hz. (c) Load peak current and transferred charge density for a generator vs. frequency at P= $6.67x10^3$ Pa. (d) Load peak current and transferred charge density for a generator vs. applied pressure at f = 5 Hz. (e) Load peak current and transferred charge density for a generator upon

continuous operations up to 90000 cycles, at P= 6.67 x10^3 Pa and f= 5 Hz. Reproduced (Adapted) with permission. [64]Copyright 2017, Nano Energy.

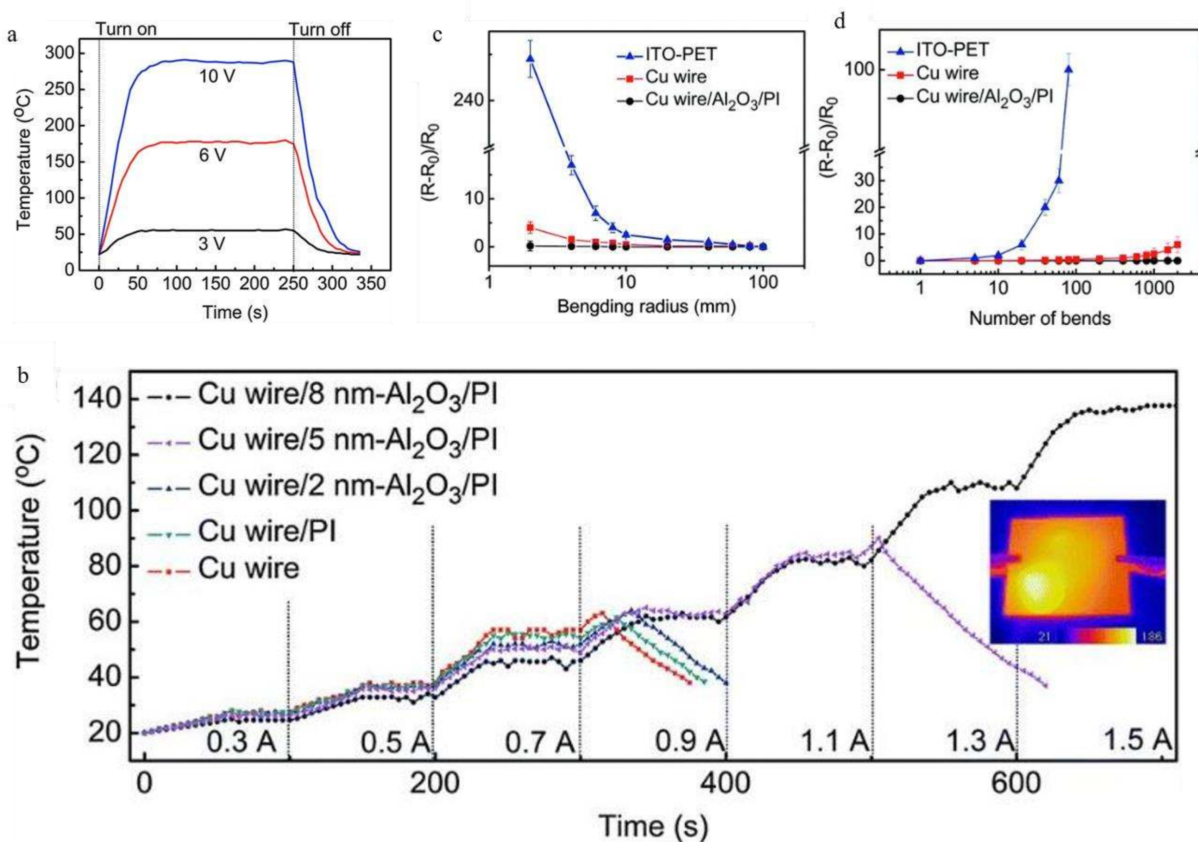

FIGURE 7: (a) Time-dependent temperature profile of the Cu wire/Al_2O_3/PI -based heaters operated at different input voltages. (b) Transient temperature response of the heaters made of different composite film under DC current sweep. The inset is an infrared thermal image of the Cu wire/8nmAl_2O_3/PI-based heater at an input current of 1.5A. (c) The resistance change vs. bending radius. (d) The resistance change vs. bending cycles with radius of 2 mm. Reproduced (Adapted) with permission. [93] Copyright 2016, Materials Chemistry C.

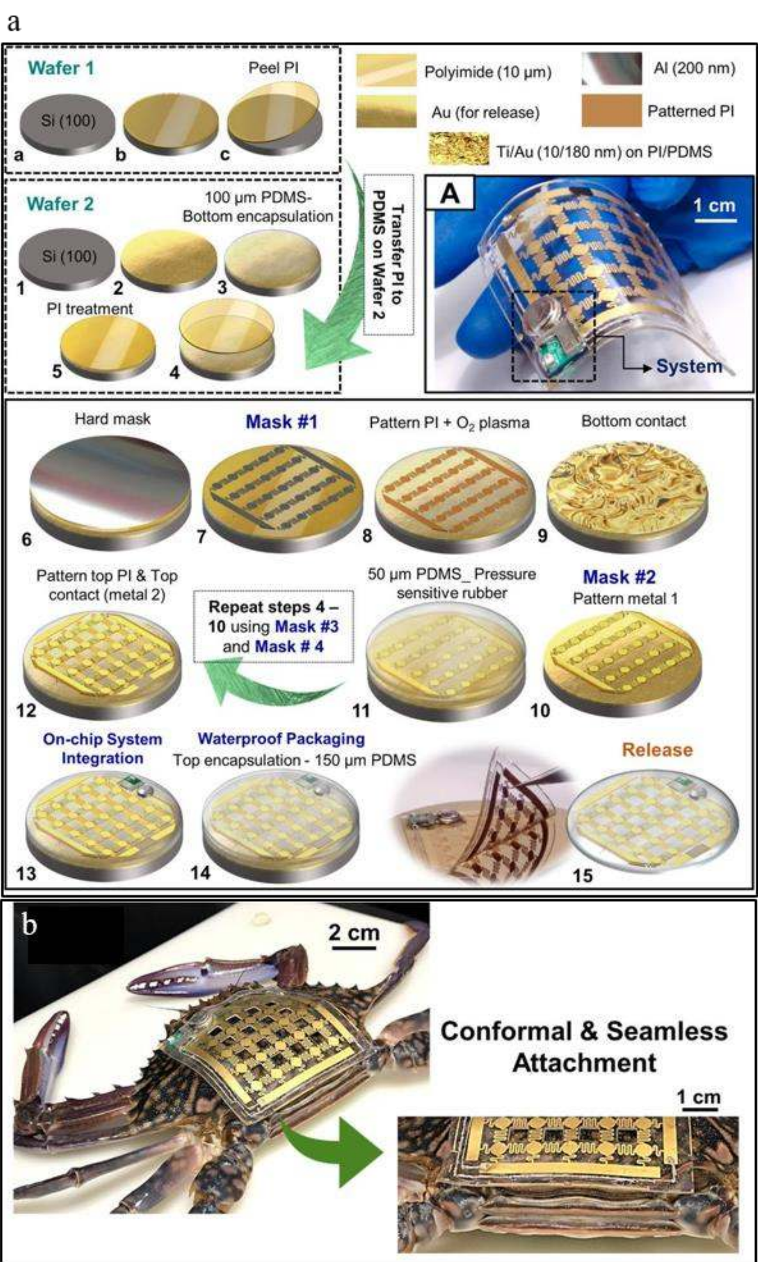

Figure 8: (a) Fabrication flow of the flexible marine skin. (b) Optical image of the marine skin attached to the crab. Adopted with permission. [10] Copyright 2018, npj Flexible Electronics.

Click here to access/download
Production Data
Main Article.doc